Facile co-precipitation synthesis of ZnO-NiO nanocomposites: fabrication, structural analysis, and assessing the impacts of various solvents on the photoabsorption, photoemission, photocatalytic, electrochemical sensing behaviour, and antibacterial activity

R.K. Shynu[a], S. Gnanam[a*], J. Gajendiran[b], J. Ramana Ramya[c], G. Thennarasu[d], S. Gokul Raj[e], G. Ramesh Kumar[f]

[a*]Department of Physics, School of Basic Sciences, Vels Institute of Science, Technology & Advanced Studies (VISTAS), Pallavaram, Chennai-600 117, India.

[b]Department of Physics, Vel Tech Rangarajan Dr. Sagunthala R&D Institute of Science and Technology, Avadi, Chennai 600 062, India

[c]Department of Periodontics, Saveetha Dental college and hospitals, Saveetha Institute of Medical and Technical Sciences, Chennai 600077

[d]Department of Chemistry, C. Kandaswami Naidu College for Men, Annanagar, Chennai-102

[e]Department of Physics, C. Kandaswami Naidu College for Men, Annanagar, Chennai-102

[f]Department of Science and Humanities, University College of Engineering Arni, Anna University Chennai, Thatchur, Arni 632 326, India

Corresponding author email: gnanam.nanoscience@gmail.com, gaja.nanotech@gmail.com

Abstract

The zinc oxide-nickel oxide (ZnO-NiO) precursor salt was dispersed separately in the distilled water-mono hydric alcohols (methanol, ethanol) and distilled water solvent mediums via a co-precipitation route and then calcined at 450^{o}C for 2 hrs to develop the zinc oxide-nickel oxide nanocomposites (ZnO-NiO, sample code ZONO-NC). The obtained final products were assessed using XRD and FE-SEM studies, which revealed distinct crystal structures (hexagonal phase of ZnO and cubic structure of NiO) and bi-type surface morphology. The surface structure, optical absorption edges, band gap values, PL emission, and specific capacitance values of the synthesized ZONO-NC results all varied significantly. The above-mentioned solvent-induced changes in properties instigate in the chemical reaction system of the zinc-nickel salt precursor solution. For suitable supercapicitor's behaviour, the synthesized ZONO-NC was used as a working electrode to examine their current responses with respect to increasing scan rates potential from 10 to 100 mV/s, and the electrochemical performance are discussed in detail. Three different dyes (Orange G, Amidoblack 10B, and Direct Blue 71) were introduced with the synthesized water-methyl alcohol assisted ZONO-NC sample as a photocatalyts in the aqueous solvent, and their photocatalytic degradation efficiency was compared. The microbial efficacy of the synthesized nanocomposite was examined by taking Staphylococcus aureus and Escherichia coli strains.

Keywords: Composite; Structural properties; Optical properties; Electrochemical properties; Photocatalytic activity; Antibacterial properties

1. Introduction

Many researchers have investigated the crystal structure, optical band gap, photoabsorption and photoemission, catalytic activity, electrochemical sensing behaviour, and antibacterial activity of individual ZnO and NiO nanostructured compounds using various bottom-up approaches [1-9]. Based on the aforementioned literature, some significant opto-chemical property results, semiconductor type, and crystal structure are consolidated and shown in Table 1. According to Table 1, the properties of ZnO and NiO nanostructures could be used to design optoelectronic devices, supercapacitors, waste water treatment, and biological applications [1-9]. Many web reports demonstrated that when n-type semiconductor (ZnO) and p-type semiconductor (NiO) composites were mixed together, they exhibited unusual opto-catalytic properties and electrochemical sensing responses when compared to individual ZnO and NiO compounds [21-27]

Table 1: The semiconductor type, crystal structure, and opto-chemical properties of nanostructured ZnO and NiO materials [1-9].

Properties	ZnO	NiO
Type of semiconductor	n-type	p-type
Crystal structure	Hexagonal	Face centered cubic
Energy gap type	Broad	Broad
Optical absorption	UV region	UV region
PL emission	UV and visible region	UV and visible region
Catalytic activity	Highly active surface lattice	Highly active surface lattice
Chemical and thermal stability	Good	Good
Electrochemical sensing behaviour	Fast charge and discharge response	Fast charge and discharge response

The chemical synthesis techniques, particle shape, photocatalyst dye, light source, and photodegradation efficiency of as-obtained ZONO-NC are compared to the reported values [10-22] which are summarized in Table 2. When compared to previously reported work, Table 2 shows that ZONO-NC has higher photocatalytic degradation efficiency.

Table 2: Comparative parameters of prepared ZONO-NC compounds.

Material	Chemical synthesis method	Particle shape	Photocatalyst dye	Light source	Photo degradation efficiency	References
ZnO-NiO	Hydrothermal & ultrasonic spray pyrolysis	Hexagonally-nanorods	Methylene Blue (MB)	UV light	~70 %,	Chen et al. [10]
ZnO-NiO	Precipitation method	Round shaped nanoisland	MB	Solar light	79.76	Yousaf et al. [11]
ZnO-NiO	Co-precipitation &	Spherical	MB, Rhodamine-B	Solar light	49.6%	Aziz et al.

	ultrasonication		(RhB), Benzoic acid,		77% 88.1%	[12]
ZnO-NiO	Electrospun	Nanofibers	MB	Visible light	65%	Kanjwala et al. [13]
ZnO-NiO	Sol-gel synthesis	Mesoporus	MB	UV and sun light		El-Katori et al. [14]
ZnO-NiO	Precipitation method	Spherical/cubic structure	Aniline blue (AB), brilliant green (BG) direct red 80 (DR 80)	Sun light and UV light	85 76 60	Muhambihai et al. [15]
NiO-ZnO composite	Solvothermal method	Flower like structure	Tetracycline	Visible light	92%	Hui et al. [16]
NiO-ZnO composite	chemical bath deposition	Cubic/flower like structure	Methyle Orange (MO)	UV light	99%	Tian et al. [17]
ZnO-NiO	Ultrasonic-assisted method	Spherical	RhB, MB, MO	UV light	-	Taghizadeh et al. [18]
ZnO-NiO	Sonochemical	Spherical	MB	Solar light	89%	Udayachandran Thampy et al. [19]
ZnO-NiO	Electrochemical deposition on carbon fiber cloth substrates	Nanorods/Nanosheets	RhB & MO	UV light	95%	Ding et al. [20]
ZnO-NiO	Pulse electrodeposition followed by thermal oxidation	Nanoneedle	RhB	UV light	48%	Wu et al. [21]
NiO-Decorated ZnO	Precipitation	Nanowhiskers	MB	UV light	72%	Abdul Rahman et al. [22]
ZnO-NiO	Co-Precipitation	rods/spherical	Orange G, Amidoblack 10B, Direct Blue 71	Visible light	97% 97% 94%	This current work

Furthermore, Table 3 compares the reported specific capacitance (C_{spec}) values of as-synthesized ZnO-NiO by various chemical routes [23-27] with the current work. According to Table 3, the synthesised ZONO-NC has moderate electrochemical sensing behaviour, is cost-effective, easily forms precipitation after mixing metal salt with precipitation agent in the solvent medium, and has a lower processing temperature.

Table 3: Chemical synthesis techniques, particle shape, and specific capacitance values of the reported ZnO-NiO composite were compared with the present work.

S. no	Material	Chemical synthesis techniques	Particle shape	Specific capacitance (F g^{-1})	References
1	NiO-ZnO composite	Hydrothermal	Mesoporous	1394C g^{-1} at a current density of 1 A g^{-1}	Wang et al. [23]
2	ZnO-NiO	Hydrothermal	Hexagonal nanorod	665.4 at a current density of 1 A g^{-1}	Nagaraju et. al [24]
3	ZnO-NiO	Chemical bath deposition (CBD)	Nanosheet	1248	Chebrolu et al. [25]
4	ZnO-NiO	CBD	Micropolyhedrons	649	Pang et. al [26]
5	ZnO-NiO	Wet-chemical synthesis	Nanorods	132 at current density of 2 Ag^{-1}	Zheng et al. [27]
6	ZnO-NiO	Co-precipitation method	Spherical/nanorods	92 to 195 at a scan rate potential 10 mV/S	This current work

To date, no report of ZONO-NC has been made using the co-prescipitation route with the assistance of four different solvent mediums such as distilled water-mono hydric alcohols (methanol, ethanol) and distilled water followed by testing the powder XRD, SEM, UV, PL, and cyclic voltammetric characterization, and their finding results are discussed comparatively in detail. The chemically attached elements, dispersed particle shape and zone diameter of inhibition of synthesized water-methyl alcohol assisted ZONO-NC have been identified using EDX, TEM and antibacterial activity studies. To the best of our knowledge, three different dyes (Orange G, Amidoblack 10B, and Direct Blue 71) were introduced with synthesized water-methyl alcohol assisted ZONO-NC as photocatalysts in the aqueous solvent, and their photocatalytic degradation efficiency is comparatively investigated in detail for the first time.

2. Experimental

A clear solution was made through dissolving 2.215 g of white solid salt of dicarbomethoxyzinc and 2.14 g of green solid salt of nickel (II) acetate in a separate beaker containing 100 mL of mixture solvents such as water and methyl alcohol (1:1 ratio) under magnetic stirring. Subsequently, 0.2 g of caustic soda pellets was added to the above mixture solution. The resulting mixture solutions were heat-treated for 18 hrs at 150^{o}C. Furthermore, the obtained products were washed several times with ethanol to remove impurities. Finally,

zinc oxide (ZnO)/nickel oxide (NiO) composites were obtained when the above filtered product sample were calcined at 450^{o}C for 2 hrs. The same procedure was used to prepare ZONO-NC using methyl alcohol, ethyl alcohol, and water as solvents instead of a mixture solvent (water-methyl alcohol). The characterization of the synthesized ZONO-NC compounds can be found in the supporting information.

3. **Results and Discussion**

3.1 Powder XRD analysis of the ZONO-NC

The recorded diffraction peaks of the synthesized various solvent assisted ZnO-NiO composites using powder XRD instrument are viewed in Fig.1 (a-d). The obtained diffraction patterns were examined with the reported powder XRD peaks of the ZnO-NiO material, followed by strong diffraction peaks indexed in the XRD, which confirms the hexagonal phase of zinc oxide (JCPDS File No. 80-0075) and the cubic structure of nickel oxide (JCPDS File No. 78-0429) were successfully formed [15].

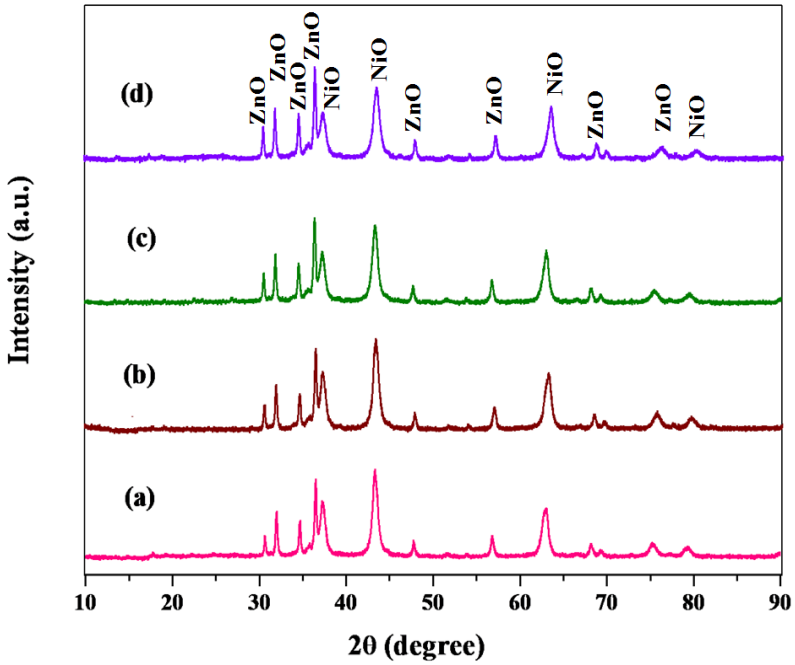

Fig.1 XRD pattern of the ZONO-NC (a) distilled water-methanol, (b) methanol, (c) ethanol, and (d) distilled water solvents.

3.2 FE-SEM studies of the ZONO-NC

The internal surface microstructures of the synthesized ZONO-NC were assessed with the aid of FE-SEM studies. The SEM image of the distilled water-methanol mixture solvents assisted ZONO-NC revealed two different particle shapes (rods and spherical) (Fig. 2(a)). For the methanol assisted ZONO-NC (Fig. 2(b)), a large aggregation of spherical particles with a non-uniform size of rods is distributed over the surface. The SEM image of ethanol and distilled water (Fig. 2(c) and 2(d)) assisted ZONO-NC revealed only spherical particles. Furthermore, the mixture solvents (distilled water-methanol) served as a surface modifier and also regulated the distance between zinc and nickel particles from aggregation during the organic removal stage.

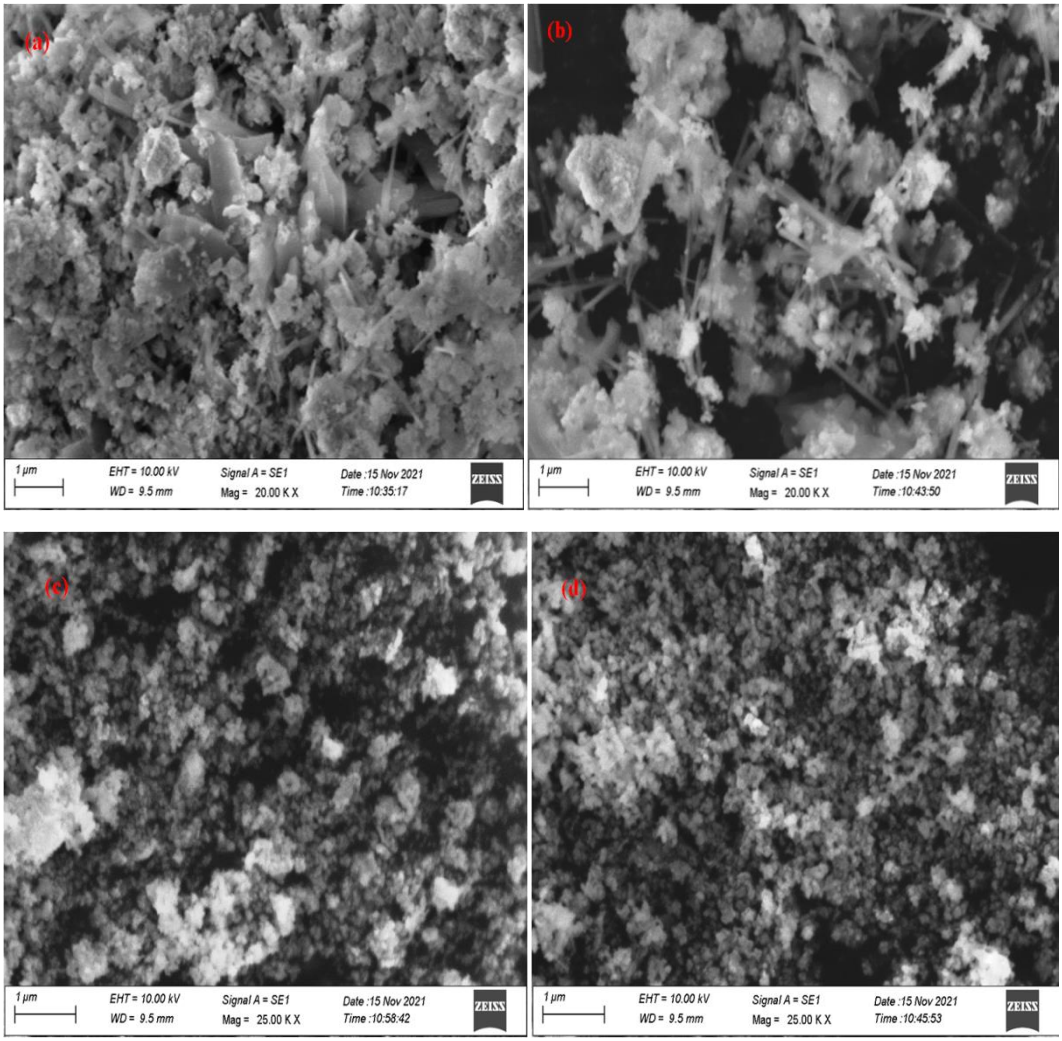

Fig.2 SEM images of the ZONO-NC (a) distilled water-methanol, (b) methanol, (c) ethanol, and (d) distilled water solvents.

3.3.TEM and EDX study of the ZONO-NC

The TEM image of distilled water-methanol mixture solvents assisted ZONO-NC revealed hetero-structure morphology consisting of nanorods and spherical particles (Fig.3 (a)). The TEM image shows bi-type morphology, indicating that both ZnO and NiO were formed. This TEM study displayed the above morphology, which is supported by the SEM results of distilled water-methanol mixture solvents assisted ZONO-NC. The chemically attached elements in the synthesised distilled water-methanol assisted composite sample were examined using EDX analysis. The EDX spectrum was used to trace the Zn, Ni, and O elements, as well as their corresponding chemical compositions of 42.06, 30.71, and 24.13 Wt%, respectively. In addition, the carbon element was traced due to the grid.

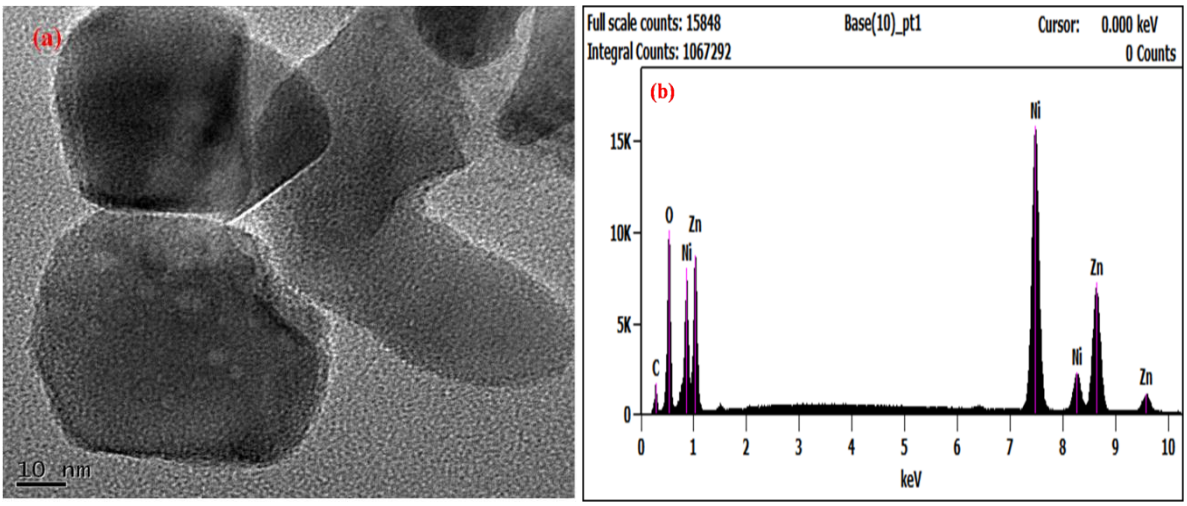

Fig.3 (a) TEM image and (b) EDX of the distilled water- methanol assisted ZONO-NC.

3.4 UV-visible spectra analysis of the ZONO-NC

With the aid of UV-visible spectra analysis, each solvent assisted ZONO-NC sample was tested for optical absorbance (Fig.4 (a-d)), and optical band gap values (Fig.4 (e-h)). All obtained ZONO-NC samples had a broad light absorption peak in the ultra-violet portion [17, 21]. Following a thorough examination of the preceding studies, significant variations in optical absorbance and band gap values were discovered for the aforementioned ZONO-NC compounds under the influence of various solvents. Furthermore, optical band values are measured in two different places, indicating that the mixed compounds are present. The detected optical band gap values of all ZONO-NC from the Tauc plot (Fig.4 (e-h)) are consolidated in Table S1 (Supporting Information).

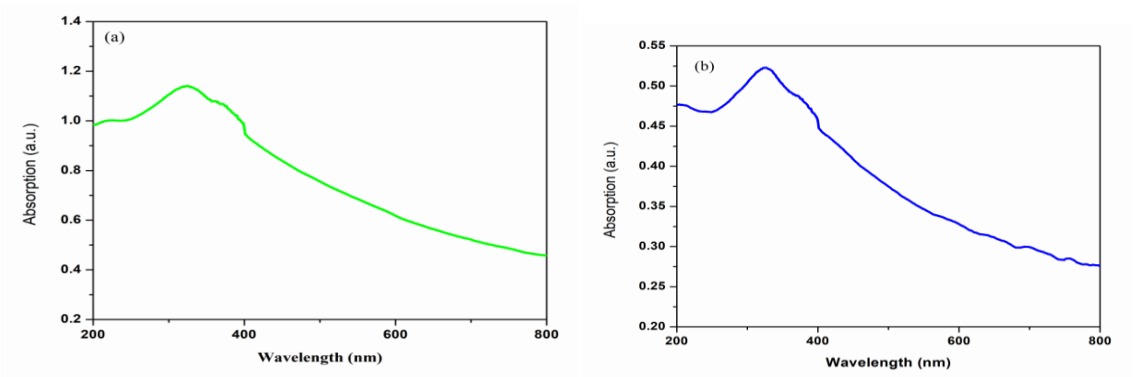

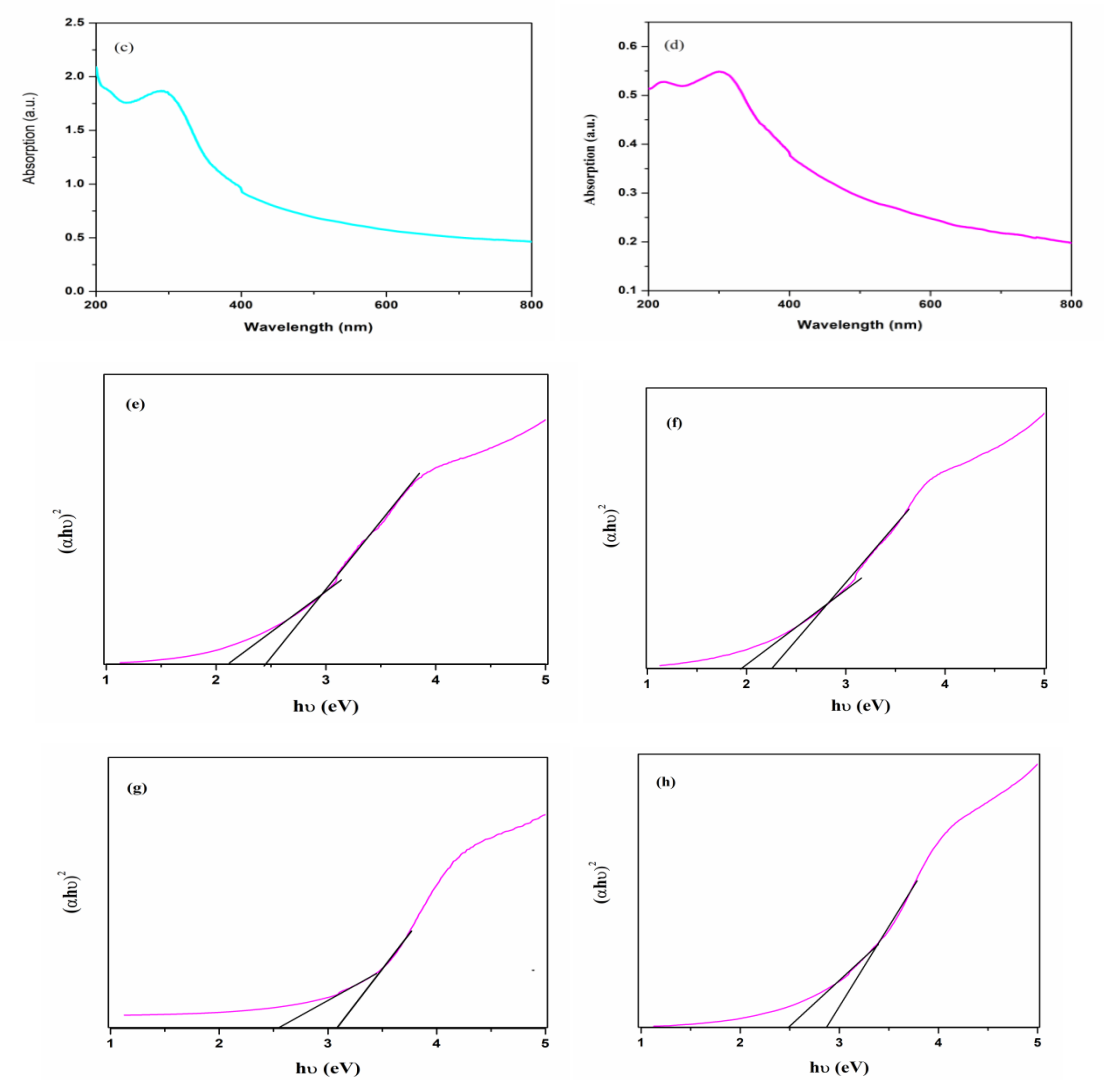

Fig.4 UV-visible spectra of the ZONO-NC (a) distilled water- methanol, (b) methanol, (c) ethanol, and (d) distilled water solvents and corresponding tauc plot (e-h).

3.5 PL Analysis of the ZONO-NC

The PL spectra of synthesised ZONO-NC samples revealed a weak visible emission peak at 425 nm, as shown in Fig.6. The detected visible emission peaks indicate that they are caused by structural or oxygen vacancy defects. For all ZONO-NC samples, there was no significant PL emission shift. Further, no UV emission was detected in the PL spectra of ZONO-NC samples. The observed PL emission behaviour of ZONO-NC differs from the previously reported PL emission of ZnO-NiO composite [19, 20].

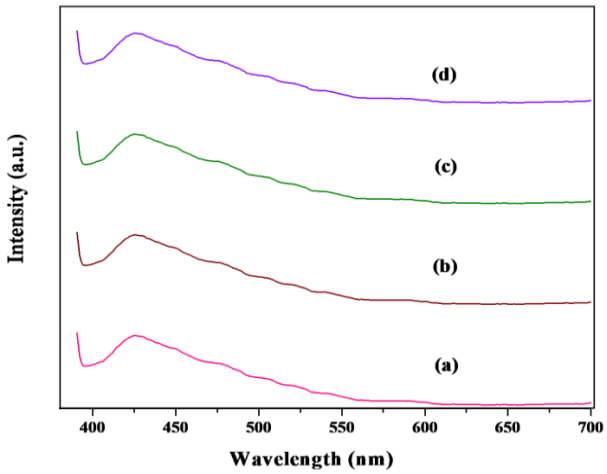

Fig.5 PL spectra of the ZONO-NC (a) distilled water-methanol, (b) methanol, (c) ethanol, and (d) distilled water solvents.

3.6 CV analysis of the ZONO-NC

Different scan rates (10, 20, 30, 50, 60, 80, and 100 mV/s) were applied in the potential range of -2.5 to 2.5 V to record the electrochemical sensing activity results of as-synthesized ZONO-NC samples, which are presented in Fig. 6. By applying scan rates changing from 10-100 mV/s to all ZONO-NC samples, it is deduced that current values vary significantly. In addition, the oxidation and reduction peaks were clearly shifted depending on the tuning of various scan rates for all ZONO-NC samples. This observed phenomenon is attributed to the faradic reaction [28]. The characteristics mentioned above would be useful in the application of supercapacitors. Furthermore, Pang et al. [26] found that increasing scan rates of ZONO-NC increased current loop areas significantly.

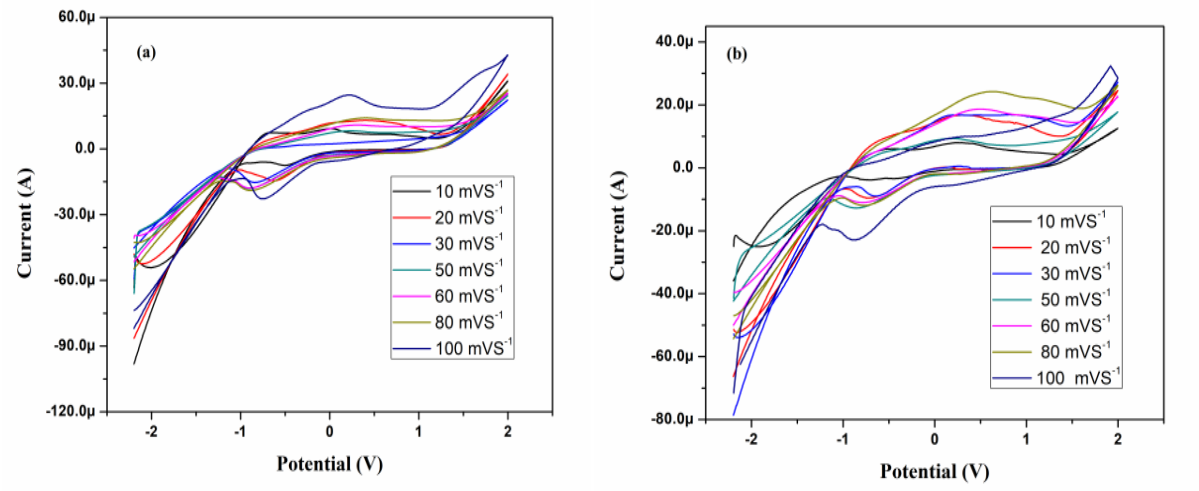

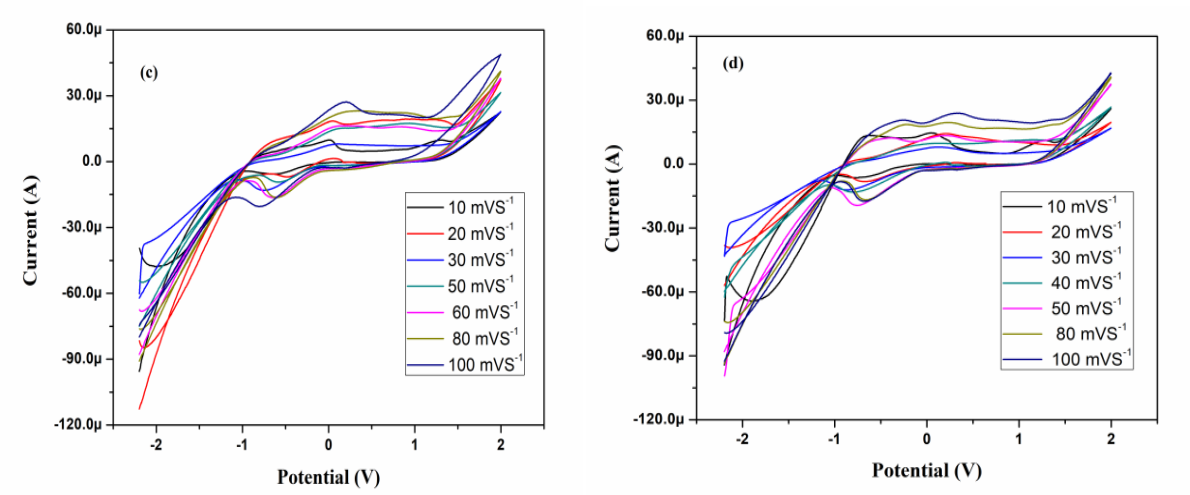

Fig.6 CV graphs of the ZONO-NC (a) distilled water-methanol, (b) methanol, (c) ethanol, and (d) distilled water solvents.

The detected current response values from the CV graphs, as well as specific capacitance values, are calculated using the $C_{sp} = \int I\, dv/(mv\, \Delta V)$ formula, and the results are summarized in Table S2 (Supporting Information). The calculated specific capacitance values of synthesized ZONO-NC samples, comparable with the reported specific capacitance values of ZnO-NiO composites [23-27].

3.7 Photocatalytic activity of the ZONO-NC

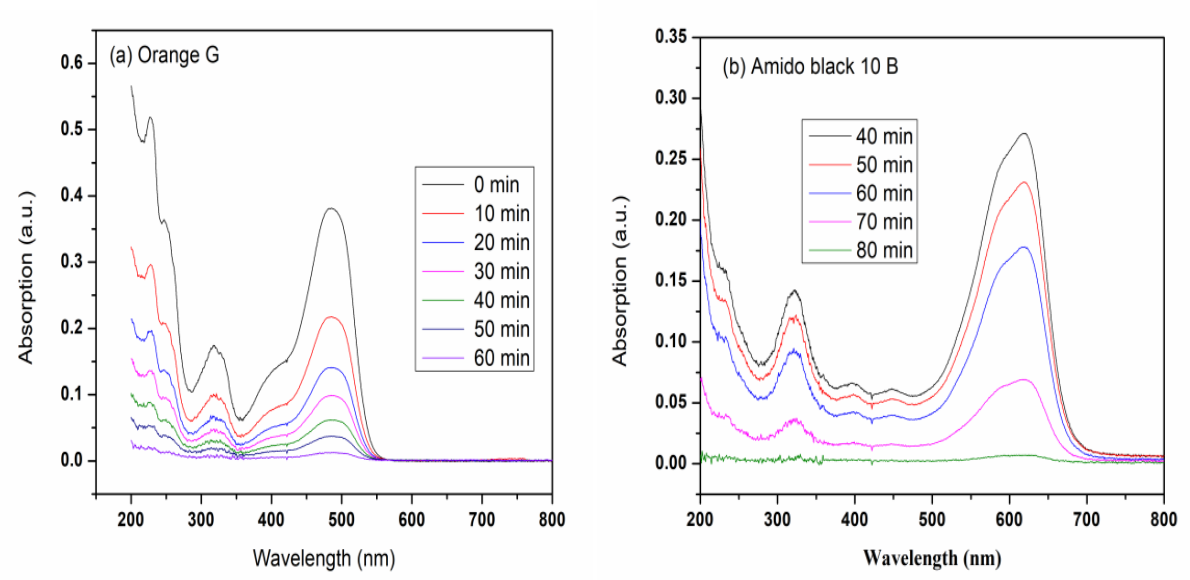

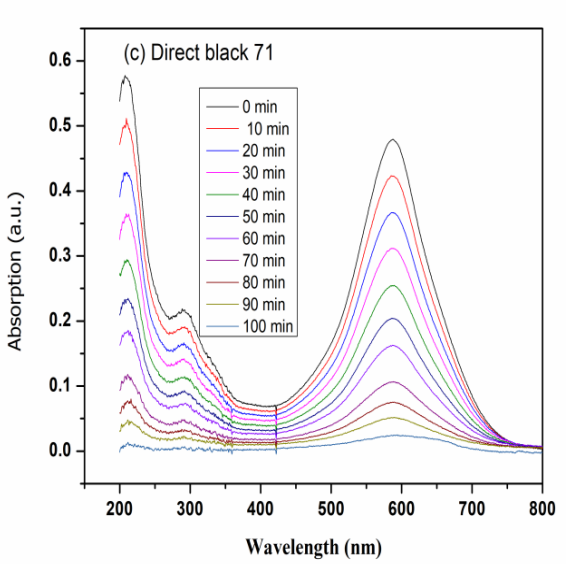

Fig.7 Catalytic activity of the distilled water-methanol assisted ZONO-NC as a photocatalyst in the presence of different dyes (a) Orange G, (b) Amidoblack 10B and (c) Direct Blue 71.

In the current investigation of photocatalytic activity studies, water-methyl alcohol solvent assisted ZONO-NC as a photocatalyst was dispersed in the aqueous medium along with Orange G, Amidoblack 10B, and Direct Blue 71 as three different dyes were followed by photodegradation activity recorded through UV-visible spectra and are displayed in Fig.7. Following a careful examination of the obtained optical absorption spectra graphs, the optical absorption wavelength of chromophore and aromatic part was discovered and is given in Table S3 (Supporting Information).

Some significant findings can be drawn from Fig.7 as follows: (i) chromophore group decreases with increasing irradiation time-decolorization confirmed, and (ii) aromatic group decreases with increasing irradiation time-degradation confirmed. In addition, the photocatalytic efficiency of the ZONO-NC with various dyes is given in Table.S4 (Supporting Information). According to the photocatalytic efficiency results in Table S4, monoazo dye (Orange G) has better photo degradation than diazo and triazo dyes because diazo dye has two N=N groups and triazo dye has three N=N groups, whereas monoazo dye has only one N=N group.

3.8 Antimicrobial Activity of the ZONO-NC

Fig. 8 depicts the antimicrobial activity of the water-methyl alcohol solvent assisted ZONO-NC results. The agar well diffusion method was employed to investigate the microbial efficacy of the ZONO-NC versus gram-positive (Staphylococcus aureus) and gram-negative (Escherichia coli) strains. The positive control is streptomycin, and the negative control is distilled water. The diameter of the zone of inhibition was measured to be 2.7 ± 0.3 cm and 2.3 ± 0.2 cm, respectively for E. coli and S. aureus, in the positive control. There was no inhibitory zone in the negative control. The inhibitory zones were measured after a 100 µg/mL ZONO-NC sample was suspended in agar wells for 24 hrs.

Mechanisms of inhibition for gram-positive and gram-negative strains differ. Gram-negative bactericidal activity is caused by interference with various metabolic pathways,

whereas gram-positive bactericidal activity is caused by interference with DNA replication and transcription [29]. Gram-negative bacteria have carbohydrates, lipids, and lipopolysaccharide layers on their cell walls, whereas gram-positive do not [30, 31]. The ZnO-NiO present in the sample could be responsible for the bacteria's inhibitory effect. The major causes of the binary oxide of metal's bactericidal behaviour are cell wall disruption, binding of bi-metal oxide to DNA and proteins, ROS generation, interference with bacterial DNA replication, and changes in the bacteria's genes [32]. The antimicrobial activity against both strains is owing to the release of Zn^{2+} and Ni^{+2} ions. These ions attach to the bacterial cell wall via electrostatic interactions and rupture it. Then, it penetrates the bacterial cell wall, resulting in the generating of Reactive Oxygen Species (ROS) and the disruption of the microbe's respiratory chain. ROS such as hydroxyl, oxygen, hydrogen peroxide, and superoxide anions are responsible for the formation of excess free radicals, which damage the internal components of the bacterial cell and eventually kill it.

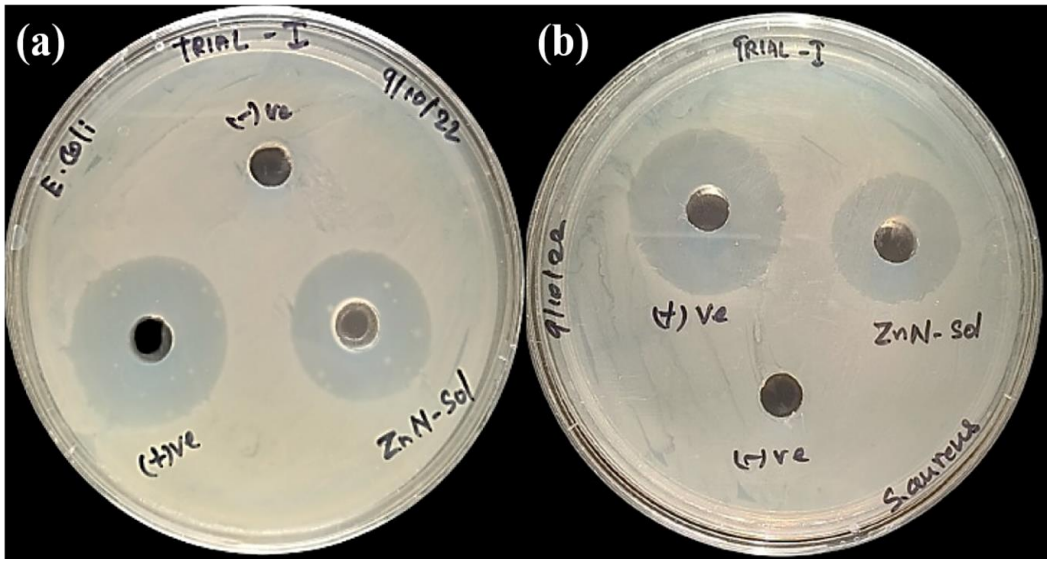

Fig.8 The antimicrobial activity of the distilled water- methanol solvent assisted ZONO-NC.

4. Conclusions

Distilled water- methanol, methanol, ethanol, and distilled water solvents medium assisted ZONO-NC were synthesized through the co-precipitation route. Powder XRD analysis was used to identify the mixed crystalline structure (i.e., ZnO-NiO). Solvents were used to tune the surface structures, optical absorption, and band gap values of ZONO-NC samples. EDX analysis was used to trace the individual elements of the ZONO-NC. For all ZONO-NC samples, the PL emission results revealed a weak visible peak with no significant PL emission shift. The tuning of current responses, and redox peak shift of the ZONO-NC electrode were observed with the varying scan rates from 10 to 100 mV/s through confirmed cyclic voltammetric studies. The photocatalytic results show that Orange G (monoazo dye) has better photo degradation than Amidoblack 10B and Direct Blue 71 dyes. The

chromospheres and aromatic groups decrease with increasing irradiation time, as determined by the recorded absorption spectral graphs, and decolorization and degradation are confirmed as a result. Antibacterial studies revealed that the positive control E. Coli had a larger zone of inhibition than the positive control S. aureus and the negative control.

References

[1] Ayesha Ahmed Sumra, Muhammad Aadil, Syeda Rabia Ejaz, SaimaAnjum, TahiraSaleem, MaryamZain, Ibrahim A.Alsafari, Ceramics International. 48 (2022) 14652-1466.

[2] Smita Dey**,** Souvik Das**,** Asit Kumar Kar, Materials Chemistry and Physics**.** 270 (2021) 124872.

[3] F. M.Sanakousar**,** C.C.Vidyasagar**,** V.M.Jiménez-Pérez**,** K.Prakash, Materials Science in Semiconductor Processing**.** 140 (2022) 106390.

[4] M.A.Alvi, A.A.Al-Ghamdi, M. Shaheer Akhtar, Materials Letters. 204 (2017) 12-15.

[5] E. IndrajithNaik**,** H.S. BhojyaNaik**,** R.Viswanath**,** B.R.Kirthan**,** M.C.Prabhakara, Chemical Data Collections, 29 (2020) 100505.

[6] Mohd Arif, AmitSanger, Mohd.Shkir, ArunSingh, R.S.Katiyar, Physica B: Condensed Matter.552 (2019) 88-95.

[7] Muhammad AhsanShafique**,** Zeeshan Zaheer**,** G.Murtaza**,** T.Hussain**,** Saqlain A.Shah**,** A.N.Akhtar**,** R.Ahmad, Optik. 267 (2022) 169634.

[8] S.Prabhu, T.Daniel Thangadurai, P.Vijai Bharathy, Pon.Kalugasalam, Results in Chemistry. 4 (2022) 100285.

[9] Rajesh Vyas**,** Kumar Navin**,** Gagan Kant Tripathi**,** Rajnish Kurchania, Optik**.** 231 (2021) 166433.

[10] Zengjun Chen, Tatjana Dedova, Nicolae Spalatu, Natalia Maticiuc, Marin Rusu, Atanas Katerski, Ilona Oja Acik, Thomas Unold, Malle Krunks**,** Colloids and Surfaces A: Physicochemical and Engineering Aspects 648 (2022) 129366.

[11] Sheraz Yousaf , Sonia Zulfiqar, Muhammad Imran Din,Philips O. Agboola, Mohamed F. Aly Aboud, Muhammad Farooq Warsi, Imran Shakir, J. Mater. Res. Tech. 12 (2021) 999-1009.

[12] Fatima Aziz, Hala M.Abo-Dief, Al-zoha Warsi, Muhammad Farooq Warsi, Muhammad Shahid, Taloot Ahmad, Gaber A.M.Mersal, Mohamed M.Ibrahim, Physica B: Condensed Matter. 640 (2022) 413858.

[13] Muzafar A. Kanjwal, Ioannis S. Chronakisa, Nasser A.M. Barakat, Ceramics International. 41 (2015) 12229-12236.

[14] Emad E.El-Katori, Ensaf Aboul Kasim, Doaa A.Ali, Colloids and Surfaces A: Physicochemical and Engineering Aspects. 636 (2022) 128153.

[15] P.Muhambihai, V.Rama, P.Subramaniam, Environmental Nanotechnology, Monitoring & Management. 14 (2020) 100360.

[16] Shushu Chu, Hui Li, Yingzi Wang, Qian Ma, Hang Li, Qi Zhang, Ping Yang, Materials Letters. 252 (2019) 219-222.

[17] Fengshou Tian, Yanli Liu, Scripta Materialia. 69. (2013) 417-419.

[18] Mohammad Taghi Taghizadeh, Faezeh Nejhad-babaie Kheljan, Morteza Vatanparast, Journal of Materials Science: Materials in Electronics. 29 (2018) 978–984.

[19] U.S. Udayachandran Thampy, A. Mahesh, K. S. Sibi, I. N. Jawahar, V. Biju, SN Applied Sciences.1 (2019) 1478.

[20] Meng Ding, Hongcen Yang, Tian Yan, Chenggang Wang, Xiaolong Deng, Shouwei Zhang, Jinzhao Huang, Minghui Shao & Xijin Xu, Nanoscale Research Letters. 13 (2018) 260.

[21] Jun Wu, Chengzhi Luo, Delong Li, Qiang Fu, Chunxu Pan, Journal of Materials Science. 52 (2017) 1285-1295.

[22] I. Abdul Rahman**,** M. T. M. Ayob, S. Radiman, Enhanced Photocatalytic Performance of NiO-Decorated ZnO Nanowhiskers for Methylene Blue Degradation, J. Nanotechnology. (2014) 212694.

[23] Tianyang Wang, Jie Liu, Yuxin Ma, Shuang Han, Changdong Gu, Jianshe Lian, Electrochimica Acta. 392 (2021) 138976.

[24] Y.S. Nagaraju, H. Ganesh, S. Veeresh, H.Vijeth, M. Basappa, M. Vandana, H. Devendrappa, Materials Science in Semiconductor Processing.142 (2022) 106429.

[25] Venkata Thulasivarma Chebrolu, Balamuralitharan Balakrishnan, Inho Cho, Jin-Soo Bak, Hee- Jee Kim, Dalton Trans. 49 (2020) 14432-14444.

[26] Huan Pang, Yahui Ma, Guochang Li, Jing Chen, Jiangshan Zhang, Honghe Zheng and Weimin Du, Dalton Trans. 41 **(**2012) 13284-13291.

[27] Xin Zheng, Kang Zhang, Yihui Sun, Sijia Jin, Yang Li, Hua Yu, Haiying Qin, Yanyan Ding, Journal of Alloys and Compounds**.** 851 (2021) 156902.

[28] Xin Zheng, Xiaoqin Yan, Yihui Sun, Zhiming Bai, Guangjie Zhang, Yanwei Shen, Qijie Liang, Yue Zhang, ACS Appl. Mater. Interfaces. 7 (2015) 2480-2485.

[29] J.K. Pandey, R.K. Swarnkar, K.K. Soumya, P. Dwivedi, M.K. Singh, S. Sundaram, R. Gopal, Applied biochemistry and biotechnology. 174 (2014) 1021-1031.

[30] Q.L. Feng, J. Wu, G.Q. Chen, F.Z. Cui, T.N. Kim, J.O. Kim, Journal of Biomedical Materials Research. 52 (2000) 662-668.

[31] K. Feris, C. Otto, J. Tinker, D. Wingett, A. Punnoose, A. Thurber, M. Kongara, M. Sabetian, B. Quinn, C. Hanna, D. Pink, Langmuir. 26 (2010) 4429-4436.

[32] Kaushik, R. Niranjan, R. Thangam, B. Madhan, V. Pandiyarasan, C. Ramachandran, D.H. Oh, G.D. Venkatasubbu, Applied Surface Science. 479 (2019) 1169-1177.